

# Whispering-gallery-mode electro-optic modulator and photonic microwave receiver

Vladimir S. Ilchenko, Anatoliy A. Savchenkov, Andrey B. Matsko, and Lute Maleki

*Jet Propulsion Laboratory, California Institute of Technology, 4800 Oak Grove Drive, Pasadena, California 91109-8099*

Received May 8, 2002

We report on the experimental observation of efficient all-resonant three-wave mixing using high- $Q$  whispering-gallery modes. The modes were excited in a millimeter size toroidal cavity fabricated from  $\text{LiNbO}_3$ . We implemented a low-noise resonant electro-optic modulator based on this wave mixing process. We observe an efficient modulation of light with coherent microwave pumping at 9 GHz with applied power of approximately 10 mW. Used as a receiver, the modulator allows us to detect nanowatt microwave radiation. Preliminary results with a 33-GHz modulator prototype are also reported. We present a theoretical interpretation of the experimental results and discuss possible applications of the device. © 2003 Optical Society of America

OCIS codes: 230.2090, 230.4110, 230.0040, 230.5750, 190.4360.

## 1. INTRODUCTION

Whispering-gallery modes play a significant role in modern nonlinear optics. High-quality factors and large field densities associated with whispering-gallery modes in dielectric resonators result in resonant enhancement of nonlinear interactions of various kinds.<sup>1–6</sup> These modes provide the opportunity to achieve a high nonlinear response with weak electromagnetic fields, even if the cavity is fabricated from a material with low nonlinearity, as is usually the case for optically transparent materials. In this way, whispering-gallery modes can also be used in applications such as all-optical switching devices,<sup>7–9</sup> microlasers,<sup>10–19</sup> and optical sensors.<sup>20–24</sup> In particular, many future communications applications such as microwave cellular phone and personal data assistant networks require devices capable of receiving, transforming, and processing signals in a millimeter wavelength domain.<sup>25</sup> Electro-optic modulators based on electromagnetic wave interaction in nonlinear optical cavities with high- $Q$  whispering-gallery modes will play an enabling role for these and similar applications.

The motivation for the optical cavity-based modulators stems from the large operating powers required to drive the existing modulators. Both broadband-integrated Mach–Zehnder modulators and free-space microwave cavity-assisted narrowband modulators typically require approximately 1 W of microwave power to achieve a significant modulation. By utilizing high- $Q$  resonances instead of zero-order interferometry or polarization rotation as the basis for electro-optic modulation one can potentially reduce the controlling power by many orders of magnitude. This, of course, is at the expense of a limited bandwidth that nevertheless is still practical for many applications.

The core of the modulator can be a cavity made with a second-order nonlinearity material, such as  $\text{LiNbO}_3$ . Optical losses in lithium niobate are small enough to allow for relatively high  $Q$ s of whispering-gallery modes.

With such modes the microwave power can be applied to a small volume, which increases the field at a given voltage but leaves a small capacitive load. This configuration allows the high  $Q$  of the cavity to be preserved. Hence, even a small voltage applied across the area of confinement of the optical field is enough to induce a change in the frequency of the whispering-gallery resonance with a magnitude comparable to its bandwidth. This forms the basis for an efficient modulation.

Most of the previous studies in this area have dealt with nonlinear cavity optics in a single-mode regime. The higher the quality factor of the cavity modes in this regime, the stronger the nonlinear interactions. However, this relationship also creates a narrow spectral range where the nonlinear interactions take place. This seriously restricts the application of the resonant nonlinearities for the enhancement of wide-band nonlinear phenomena, which include multiwave mixing, photon upconversion and downconversion, and broadband optical modulation. These applications are important for advanced, high-speed communications systems.

At first glance it might seem obvious that use of multiple modes of a nonlinear cavity will further benefit strong nonlinear interactions among electromagnetic waves of different frequency. However, such interactions usually are strongly forbidden by the momentum conservation law (phase-matching condition) because whispering-gallery modes of a rotationally symmetric dielectric resonator are orthogonal to each other in the momentum space. Interactions between these modes are possible only if the symmetry of the system is broken. Note, however, that to be useful, an artificial lifting of the symmetry should conserve the main properties of the modes, namely, their high-quality factor and small volume.

An approach to overcome this phase-matching deadlock for the three-wave mixing problem was recently proposed.<sup>20,21,26</sup> In those studies we achieved an efficient resonant interaction of several optical whispering-gallery

modes and a microwave mode by engineering the shape of a microwave resonator coupled to a microtoroidal optical cavity.<sup>27</sup> On the basis of this interaction, a new kind of electro-optic modulator was suggested.<sup>20,26,28–31</sup>

In this paper we present a detailed experimental and theoretical study of the all-resonant optical microwave interaction. We show that an efficient three-wave mixing process can be realized based on the high-quality factors of the optical whispering-gallery modes and the microwave mode. This wave mixing approach has a high saturation threshold with respect to the optical fields and a high sensitivity to the microwave field. Utilizing this, we have designed, fabricated, and tested a prototype electro-optic modulator in the X band (at 9 GHz) and have performed a preliminary study of a prototype working in the Ka band (at 33 GHz). Finally, we present data for high-efficiency light modulation with small microwave powers (1-mW modulator controlling power) and discuss the feasibility of this scheme for photonic reception of microwave signals with direct upconversion into the optical domain.

## 2. EXPERIMENT

The scheme of our experimental device is shown in Fig. 1. Light from a distributed feedback laser is sent into a spheroidal optical cavity by a coupling diamond prism. The input optical power at 1550 nm entering the coupling prism ranged from 2 to 5 mW. Total optical output efficiency of the system was limited to  $-10$  dB. The cavity was fabricated from a commercial-grade flat Z-cut LiNbO<sub>3</sub> substrate. The quality factors of the loaded modes of the cavity were measured to be  $Q = 5 \times 10^6$  (finesse  $1/T \approx 300$ ). The maximum unloaded quality factor was approximately  $Q = 5 \times 10^7$ . We believe that this value is determined by the bulk-material absorption. In this setup the laser carrier frequency is scannable within the range of  $\sim 8 \times 10^{10}$  MHz.

The basic geometric parameters of the optical cavity are shown in the inset of Fig. 1. The cavity is a disk with radius  $a = 2.4$  mm and thickness  $d = 150$   $\mu$ m. The sidewall of the disk is polished such that the cavity becomes a segment of an oblate spheroid with a large semi-axis  $a$  and a small semi-axis  $b = \sqrt{2ad} < a$ . In our case the transverse curvature diameter is approximately  $b = 180$   $\mu$ m, and the extraordinary axis of LiNbO<sub>3</sub> coincides with the symmetry axis of the cavity. The index of refraction of the prism (it is  $n_p = 2.42$  for diamond) ex-

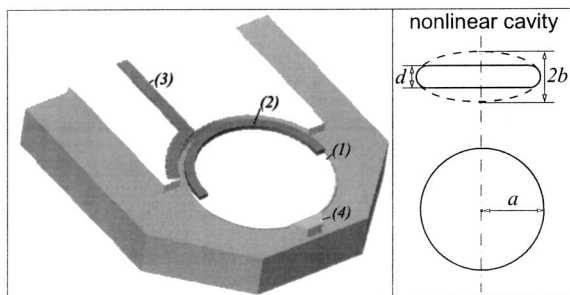


Fig. 1. Experimental setup: (1) LiNbO<sub>3</sub> optical cavity, (2) microwave resonator, (3) microwave feeding strip line, and (4) diamond coupling prism. Inset: geometric characteristics of the nonlinear optical cavity.

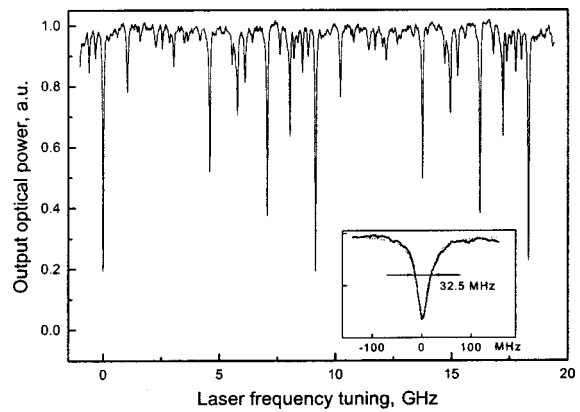


Fig. 2. Reflection spectrum of the nonlinear optical cavity. The free spectral range is 9.155 GHz. The mode quality factor is approximately  $5 \times 10^6$ .

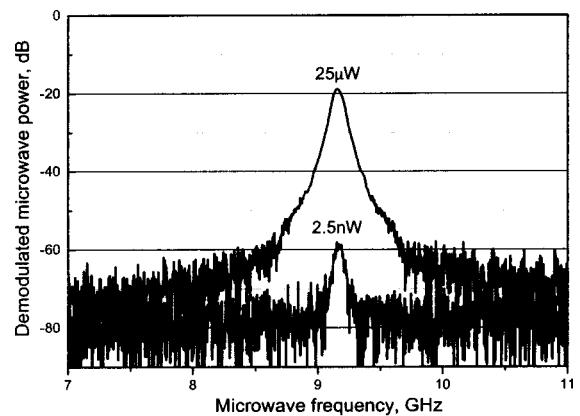


Fig. 3. Demodulated microwave power versus frequency of the microwave pumping. The zero level corresponds to the saturation power. The curve for the 2.5-nW pump was taken with 20-s averaging. This explains the lowering of the background noise level. However, even without the averaging we can see the nanowatt signals.

ceeds the effective index of refraction of the cavity whispering-gallery modes  $n = 2.14$  to create an effective coupling.

The optical cavity is placed between two electrodes of a resonator that is pumped with an external microwave source. The cavity-based modulator requires that its input light be tuned in frequency to a particular mode. Then modulation sidebands can result from the nonlinear optical excitation of adjacent Stokes and anti-Stokes modes. Because adjacent whispering-gallery modes differ in their azimuthal field dependence by exactly one period added to the closed circular waves, the microwave field applied to the resonator must not be uniform along the rim. Otherwise, the nonlinear polarization will not have any azimuthal frequency corresponding to the adjacent modes and no modulation will occur.

To tailor the microwave field configuration for optimal nonlinear interactions, we used a half-wave microstrip cavity fabricated by placing a half-circular electrode along the rim of the resonator. A typical quality factor of such a cavity is  $Q_M = 100$ , with a bandwidth of  $\sim 150$  MHz, which is sufficiently close to the bandwidth of the optical resonances. By tuning the length of the strip-line elec-

trodes, we can tune the microwave cavity to a frequency equal the optical free spectral range. The index of refraction of the lithium niobate for the microwave radiation is  $n_{mw} \approx 5$ . The spectrum of TE modes of the optical cavity is shown in Fig. 2. One can see clean mode structures with distinct individual resonance peaks and a free spectral range of 9.155 GHz. The contrast of the absorption peaks in fiber-to-fiber transmission is more than 80%.

A typical frequency response of the modulator is presented in Figs. 3 and 4. To obtain the results shown in Figs. 3 and 4, the laser frequency is kept at resonance with one of the whispering-gallery modes. The microwave frequency is then scanned, and the demodulated microwave power at the output a high-speed photodetector is recorded. The 3-dB bandwidth of the modulator is consistent with the bandwidths of the optical cavity and the microwave resonator. The two curves presented in Fig. 3 are taken well under the saturation limit shown by the 0-dB level. The smallest detectable microwave power (the sensitivity of the photonic receiver) was approximately 1 nW.

A typical spectrum of modulated signal, measured with an optical etalon for 10 mW of microwave power, is shown

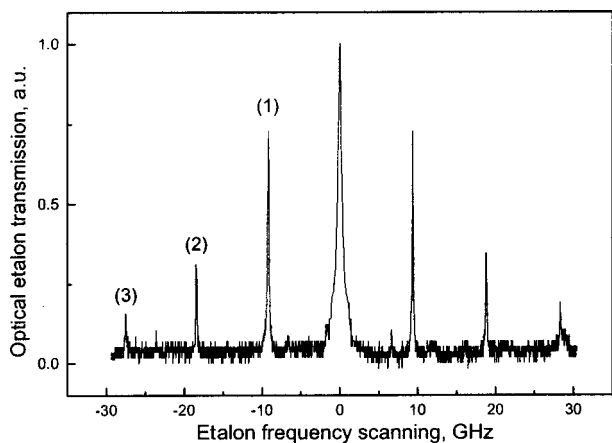


Fig. 4. Optical etalon transmission (frequency spectrum of the modulated signal) versus etalon frequency scanning. Zero frequency corresponds to the carrier frequency of pumping the system light.

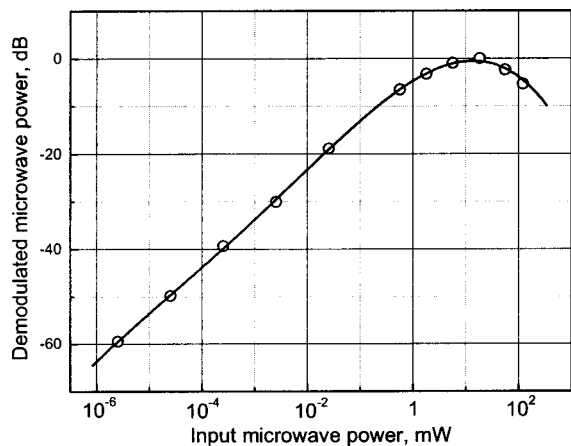


Fig. 5. Normalized demodulated microwave power versus power of the microwave pump. The absolute value of the demodulated microwave signal is approximately 30 dB less than the input microwave power.

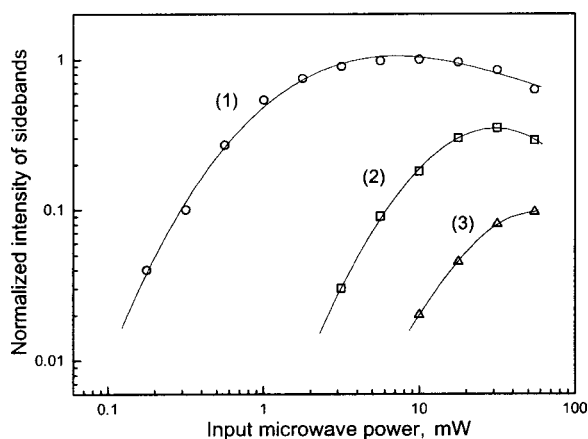


Fig. 6. Normalized power of optical harmonics generated in the modulator versus power of the microwave pump. The unity power corresponds to the maximum power of the first harmonic measured in our experiment. The curve is taken with optical etalon transmission dependence (Fig. 4).

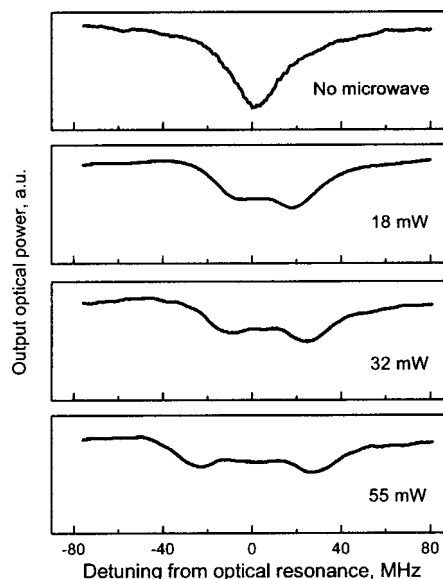


Fig. 7. Whispering-gallery-mode response curves for various powers of the microwave pump.

in Fig. 4. It is important to note that the amplitude of the central peak does not represent the total power that leaves the optical cavity. This is because approximately 20% of the pump light is reflected by the coupling prism without entering the cavity. The ratio between the generated sidebands, on the other hand, does show the actual ratio of their powers in the cavity.

The dependence of the microwave power output of the modulator on the input microwave power is presented in Fig. 5. The saturation point at  $\sim 11$  mW corresponds to the limit imposed by harmonic multiplication, as well as the power broadening of the optical resonance. The optimal operational power within the linear regime is estimated at 1 mW.

The dependence of the relative sideband power on the power of the microwave field in the resonator is shown in Fig. 6. It is easy to see that the saturation for the first sideband and the significant growth of the second and third sidebands correspond to the saturation of the de-

modulated microwave signal shown in Fig. 5. The broadening of the optical spectrum with increased microwave power is shown in Fig. 7. The width of the optical resonance increases nearly by a factor of 2 at the point of modulation saturation.

It is also interesting to check the details of the modulation in the system. To do this we measure the dependence of the demodulated microwave power on the detuning of the pump-laser frequency from the resonance with a whispering-gallery mode (Fig. 8). There is no signal at the point of exact resonance, whereas the maximum power appears for the tuning on the sloping side of the mode curve. Because the demodulated power is nonzero for amplitude-modulated light, we might say that there is no amplitude modulation for the resonant tuning of the light and the microwaves. Our theoretical calculations nevertheless predict that there is a phase modulation in this case.

Finally, Fig. 9 represents the preliminary experimental data for the *Ka*-band modulator prototype. For these data, the toroidal optical resonator has a diameter of 1.35 mm, a thickness of 120  $\mu\text{m}$ , and a transverse curvature diameter of 150  $\mu\text{m}$ . The optical free spectral range of the cavity is 33.1 GHz and the quality factor is  $\sim 10^6$ . The

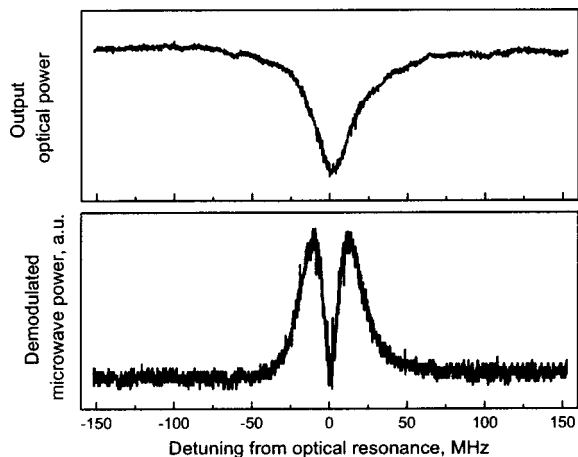


Fig. 8. Top: whispering-gallery-mode resonance. Bottom: demodulated microwave power versus detuning of the pump light from the whispering-gallery-mode resonance. No signal is found for the resonant tuning.

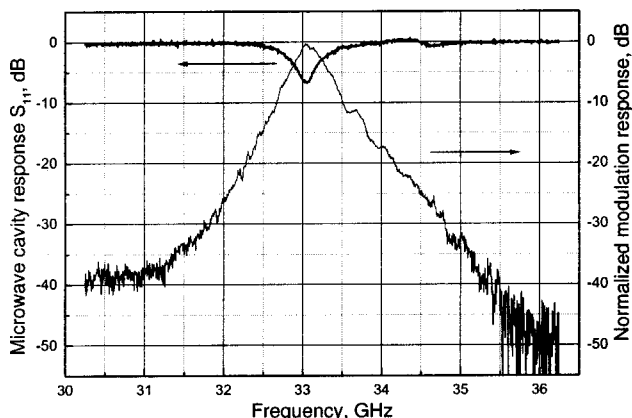


Fig. 9. Normalized demodulated microwave power versus frequency of the pump microwave field for the *Ka*-band modulation frequency.

quality factor is smaller because the cavity is in full contact with the prism coupler. The microwave cavity quality factor is approximately 60. Despite smaller dimensions and mode volumes as compared with the X-band modulator, we were unable here to reach saturation with the available maximum microwave power of  $\sim 30$  mW because of the smaller  $Q$ . In our future prototypes we expect to significantly reduce the needed microwave power through several changes such as improving the surface quality in the resonators, the introduction of a prism-resonator air gap to optimize the coupling strength, and the elimination of the extra losses in the microwave cavity.

### 3. THEORY

In what follows we briefly describe the mode structure of a dielectric spheroid and estimate the free spectral range for different kinds of mode. We then consider modes of an open cavity as independent entities (quasi-mode approach). Finally, we evaluate the problem of the interaction among three whispering-gallery cavity modes and a single mode of a microwave resonator.

#### A. Whispering-Gallery Modes

The whispering-gallery mode can be modeled as a closed circular beam supported by total internal reflections from boundaries of a dielectric cavity. A general analytic solution to describe these modes is difficult to obtain. The simplest eigenvalue and eigenfrequency problem for electromagnetic field propagation in a dielectric sphere has been solved in Ref. 32. Calculation of the spectrum of an arbitrary dielectric spheroid, however, is not a trivial task. In contrast to the case of small eccentricity,<sup>33</sup> exact analysis of a highly eccentric spheroid or toroid cannot be based on a simple approximation. To avoid complications, however, we characterize the whispering-gallery modes of a toroid following the approach introduced in Ref. 20.

A good approximation for whispering-gallery-mode eigenfrequencies in an ideal dielectric sphere with radius  $a$  much larger than the mode wavelength can be written as

$$nk_{lmq}a = t_{lq} - \frac{\xi}{(n^2 - 1)^{1/2}}, \quad (1)$$

where  $k_{lmq}$  is the mode wave number,  $t_{lq}$  is the  $q$ th zero of the spherical Bessel function of the order  $l$ , and  $n$  is the index of refraction of the material. The coefficient  $\xi$  is equal to  $n$  for TE modes and  $1/n$  for TM modes. For large orbital number  $l$ ,  $t_{lq} \approx l + O(l^{1/3})$ , it can be calculated either directly or approximated by the zeros of the Airy function.<sup>34</sup>

The second term on the right-hand side of Eq. (1) represents the fact that the dielectric cavity is open. The optical field tunnels outside the cavity surface at the characteristic length  $\sim 1/[(n^2 - 1)^{1/2}k_{lmq}]$ . The larger the refractive index  $n$ , the smaller is this length and the closer is the solution of Eq. (1) to the solution for a closed cavity.

To estimate the eigenvalues of the whispering-gallery modes in an oblate spheroid of large semiaxis  $a$ , small semiaxis  $b$ ,  $a \gg b$ , and eccentricity  $\varepsilon = (1 - b^2/a^2)^{1/2}$ , we recall that eigenfrequencies of high-order whispering-gallery modes ( $l \gg 1, m \simeq l$ ) (in an ideal sphere as well as in the spheroid) can be approximated by solutions of the scalar wave equation with zero boundary conditions. This is because most of the energy is concentrated in one component of the electromagnetic field ( $E_\theta$  for TE modes and  $E_r$  for TM modes) and the tangential component of electric field  $\mathbf{E}$  (TE modes), or the normal component of induction  $\mathbf{D}$  (TM modes) is continuous at the boundary. For the spheroid expression, similar to Eq. (1), we have

$$n\bar{k}_{mq}a = T_{mq} - \frac{\xi}{(n^2 - 1)^{1/2}}, \quad (2)$$

where  $\bar{k}_{mq} = (k_{lmq}^2 - k_\perp^2)^{1/2}$ ,  $k_\perp$  is the wave number for the angular spheroidal function and  $T_{mq}$  is the  $q$ th zero for cylindrical Bessel function  $J_m(T_{mq}) = 0$ . Because whispering-gallery modes are confined in the cavity equatorial region, we use cylindrical, not spherical, functions in our calculations.

For our purposes a rough approximation of  $k_\perp$  is enough:

$$k_\perp^2 \approx \frac{2(l - m) + 1}{a^2(1 - \varepsilon^2)^{1/2}} m. \quad (3)$$

Because  $k_{lmq} \approx l/(na)$  and  $k_\perp \approx (1 - \varepsilon^2)^{-1/4} \sqrt{l}/a$ ,  $k_{lmq} \gg k_\perp$  for our experimental parameters. Hence we can write

$$k_{lmq} \approx \bar{k}_{mq} + \frac{k_\perp^2}{2\bar{k}_{mq}}. \quad (4)$$

Substituting Eq. (2) and approximation (3) into relation (4), we finally derive

$$nk_{lmq}a = t_{lq} - \frac{\xi}{(n^2 - 1)^{1/2}} + \frac{2(l - m) + 1}{2} \left[ \frac{1 - (1 - \varepsilon^2)^{1/2}}{(1 - \varepsilon^2)^{1/2}} \right]. \quad (5)$$

Let us find the frequency splitting between two successive modes using the expression  $\omega_{lmq} = ck_{lmq}$ :

$$\begin{aligned} \omega_{l+1,mq} - \omega_{lmq} &\approx \omega_{lmq} - \omega_{l-1,mq} \\ &= \frac{c}{na} [1 + 0.62l^{-2/3} + O(l^{-5/3})], \end{aligned} \quad (6)$$

$$\begin{aligned} \omega_{l,m+1,q} - \omega_{lmq} &\approx \omega_{lmq} - \omega_{l,m-1,q} \\ &= -\frac{c}{na} \left[ \frac{1 - (1 - \varepsilon^2)^{1/2}}{(1 - \varepsilon^2)^{1/2}} \right]. \end{aligned} \quad (7)$$

Therefore by varying the geometric parameters of the cavity we are able to create an almost equidistant array of modes with a free spectral range of our choice.

The goal of our study is to achieve an efficient nonlinear coupling between each pair of neighboring modes with different numbers  $l$  by means of externally applied micro-

wave fields of the same frequency as the modes' free spectral range. We place the cavity in the microwave resonator for this purpose.

## B. Quasi-Mode Approach

We use the quasi-mode approach (see, for example, Ref. 35) to analytically describe the interaction among different modes inside a microtoroidal optical cavity. We assume that each mode in the cavity can be considered independently. This assumption is valid when the frequency splitting between the modes significantly exceeds the mode bandwidth, which is usually the case for any high- $Q$  mode of a cavity.

Let us consider a lossless cavity connected by a lossless coupler to an ideal transmission line with energy transmission coefficient  $T$  ( $1 > T$ ). The value of  $1/T$  determines the cavity finesse. The electromagnetic field  $E_{\text{in}}(t)$  in the transmission line enters the cavity through the coupler, and  $E_{\text{out}}(t)$  exits the cavity and travels in the opposite direction to  $E_{\text{in}}(t)$ . We introduce the cavity field by two electromagnetic waves propagating inside the cavity and going out of the coupler [ $E_1(t)$ ] and into the coupler [ $E_2(t)$ ].

Assuming that the coupler has a zero response time, we can write the boundary conditions on the coupler surface as

$$E_1(t) = E_{\text{in}}(t)\sqrt{T} - E_2(t)(1 - T)^{1/2}, \quad (8)$$

$$E_{\text{out}}(t) = -E_{\text{in}}(t)(1 - T)^{1/2} - E_2(t)\sqrt{T}. \quad (9)$$

Fields  $E_1$  and  $E_2$  are connected by the condition

$$E_2(t) = -E_1(t - \tau), \quad (10)$$

where  $\tau$  is the round-trip time for the cavity ( $\tau = 2\pi an/c$  for the case of a whispering-gallery mode, where  $a$  is the mode radius,  $n$  is the medium index of refraction, and  $c$  is the speed of light in the vacuum).

The set of Eqs. (8)–(10) is quite general. Let us simplify the problem and consider the case when the field inside the cavity can be presented as a product of a fast oscillating part  $\exp(-i\omega t)$  and a slow oscillating part  $\tilde{E}(t)$ , i.e.,  $E(t) = \tilde{E}(t)\exp(-i\omega t)$ . The carrier frequency  $\omega$  coincides with one of the resonant frequencies of the cavity,  $\omega\tau = 2\pi N$  ( $N$  is a real number).

We assume that the slow field amplitude inside the cavity does not change significantly during the single round-trip time. Then the expression of Eq. (10) can be expanded into a Taylor series. Keeping linear term in  $\tau$  only, we obtain

$$\tilde{E}_2(t) \approx -\tilde{E}_1(t) + \tau\dot{\tilde{E}}_1(t). \quad (11)$$

We also assume that

$$1 - (1 - T)^{1/2} \approx \frac{T}{2}. \quad (12)$$

Substituting relations (11) and (12) into Eq. (8) we obtain an equation that allows us to calculate the field inside the cavity, if we know the pump field:

$$\dot{\tilde{E}}_1(t) + \frac{T}{2\tau} \tilde{E}_1(t) = \frac{E_{\text{in}}(t)}{\sqrt{\tau}} \exp(i\omega t) \sqrt{\frac{T}{\tau}} \quad (13)$$

It is convenient to introduce a decay  $\gamma = T/(2\tau)$  and an external force  $F = E_{\text{in}}(T/\tau^2)^{1/2}$ ; then the Eq. (13) can be rewritten in the form

$$\dot{E}_1(t) + (i\omega + \gamma)E_1(t) = F(t). \quad (14)$$

Equation (14) describes the evolution of the amplitude of the field inside the cavity. For exact resonant tuning and time-independent pump field  $E_{\text{in}}$ , the ratio of light power inside the cavity  $W_1$  and outside the cavity  $W_{\text{in}}$  is  $2/(\gamma\tau)$ . The total energy accumulated in the cavity is  $W_1\tau = 2W_{\text{in}}/\gamma$ .

To find the field that exits the cavity, we use Eq. (9) that can be rewritten as

$$E_{\text{out}}(t) = -E_{\text{in}}(t) + E_1(t)\sqrt{T}. \quad (15)$$

It is worth noting that Eq. (14) describes the evolution of a single cavity mode with carrier frequency  $\omega$ . Equation (14) is valid under the conditions of relations (11) and (12). Moreover, we have to demand that the pump field  $E_{\text{in}}$  be nearly resonant with the cavity mode.

### C. Interaction of Light and Microwaves

Let us consider the problem of the nonlinear interaction of a single whispering-gallery mode pumped with radiation of a laser having carrier frequency  $\omega_0$  and a microwave field mode pumped with radiation having frequency  $\omega_M$ . We study the generation of Stokes and anti-Stokes sidebands, having  $\omega_0 - \omega_M$  and  $\omega_0 + \omega_M$  frequencies. We assume that neighboring cavity modes are nearly resonant with the sidebands.

Generally, sidebands with frequencies  $\omega_0 \pm N\omega_M$  ( $N = 1, 2, 3, \dots$ ) can be generated. We restrict our consideration to three whispering-gallery modes and a single microwave field mode and neglect the higher-order harmonics.

The Hamiltonian describing this system is

$$\hat{H} = \hat{H}_0 + \hat{V}. \quad (16)$$

$\hat{H}_0$  is the free part of the Hamiltonian:

$$\hat{H}_0 = \hbar\omega\hat{a}^\dagger\hat{a} + \hbar\omega_-\hat{b}_-^\dagger\hat{b}_- + \hbar\omega_+\hat{b}_+^\dagger\hat{b}_+ + \hbar\omega_c\hat{c}^\dagger\hat{c}, \quad (17)$$

where  $\omega$  and  $\omega_\pm$  are the eigenfrequencies of the optical cavity modes;  $\omega_c$  is the eigenfrequency of the microwave cavity mode; and  $\hat{a}$ ,  $\hat{b}_\pm$ , and  $\hat{c}$  are the annihilation operators for these modes, respectively.

The interaction part of the Hamiltonian is

$$\hat{V} = \hbar g(\hat{b}_-^\dagger\hat{c}^\dagger\hat{a} + \hat{b}_+^\dagger\hat{c}\hat{a}) + \text{adjoint}, \quad (18)$$

where

$$g = \frac{4\pi\omega}{\epsilon_a} \chi^{(2)} \left( \frac{2\pi\hbar\omega_c}{\epsilon_c\mathcal{V}_c} \right)^{1/2} \left( \frac{1}{\mathcal{V}} \int_{\mathcal{V}} d\mathcal{V} \Psi_a \Psi_b \Psi_c \right) \quad (19)$$

is a coupling constant;  $\chi^{(2)}$  is the effective second-order electro-optic constant for the material of the dielectric cavity;  $\epsilon_a$  and  $\epsilon_c$  are the dielectric susceptibilities for

the optical and microwave frequencies;  $\mathcal{V}$  is the whispering-gallery-mode volume;  $\mathcal{V}_c$  is the volume of the microwave field; and  $\Psi_a$ ,  $\Psi_b$ , and  $\Psi_c$  are the normalized dimensionless spatial distributions of the modes. We assume here that the whispering-gallery modes are nearly identical, i.e.,  $\omega \approx \omega_\pm \gg \omega_c$ ,  $\mathcal{V} \approx \mathcal{V}_\pm$ ,  $\int d\mathcal{V} \Psi_a \Psi_b \Psi_c = \int d\mathcal{V} \Psi_a \Psi_b \Psi_c$ . It should be noted here that this consideration is based on earlier studies on the subject of parametric interactions.<sup>36-38</sup>

Using the Hamiltonian in Eq. (16) we derive equations of motion for the field operators:

$$\dot{\hat{a}} = -i\omega\hat{a} - ig^*(\hat{b}_-\hat{c} + \hat{c}^\dagger\hat{b}_+), \quad (20)$$

$$\dot{\hat{b}}_- = -i\omega_-\hat{b}_- - ig\hat{c}^\dagger\hat{a}, \quad (21)$$

$$\dot{\hat{b}}_+ = -i\omega_+\hat{b}_+ - ig\hat{c}\hat{a}, \quad (22)$$

$$\dot{\hat{c}} = -i\omega_c\hat{c} - ig\hat{b}_-\hat{a} - ig^*\hat{a}^\dagger\hat{b}_+. \quad (23)$$

In reality, the optical cavity and the microwave resonator are open systems, pumped externally. Thus the pump and decay terms do not follow from the Hamiltonian approach and should be introduced in the same way as was done in Subsection 3.B. We also assume that the fields are classical, so we can neglect vacuum fluctuations leaking into the cavity. As a result, Eqs. (20)–(23) transform to

$$\dot{A} = -\Gamma_A A - ig^*(B_-C + C^\dagger B_+) + F_A, \quad (24)$$

$$\dot{B}_- = -\Gamma_{B_-} B_- - igC^\dagger A, \quad (25)$$

$$\dot{B}_+ = -\Gamma_{B_+} B_+ - igCA, \quad (26)$$

$$\dot{C} = -\Gamma_C C - igB_-\hat{A} - ig^*A^\dagger B_+ + F_M, \quad (27)$$

where

$$\Gamma_A = i(\omega - \omega_0) + \gamma,$$

$$\Gamma_{B_\mp} = i(\omega_\mp - \omega_0 \pm \omega_M) + \gamma,$$

$$\Gamma_C = i(\omega_c - \omega_M) + \gamma_M,$$

in which  $A$ ,  $B_\pm$ , and  $C$  are the slowly varying amplitudes of the operators  $\hat{a}$ ,  $\hat{b}_\pm$ , and  $\hat{c}$  respectively; the optical  $\gamma$  and microwave  $\gamma_M$  decay rates as well as pump forces  $F_A$  and  $F_M$  are introduced as in Eq. (14).

Let us solve the set of Eqs. (24)–(27) in the steady state. Neglecting the optical saturation of the microwave oscillations, we obtain from Eqs. (24) and (27)

$$A = -i \frac{g^*}{\Gamma_A} (B_-C + C^\dagger B_+) + \frac{F_A}{\Gamma_A}, \quad (28)$$

$$C \approx \frac{F_M}{\Gamma_C}. \quad (29)$$

Substituting Eq. (28) and relation (29) into Eqs. (25) and (26) in the steady state, we obtain

$$B_- = - \frac{igF_A F_M^* \Gamma_{B_+} \Gamma_C}{\Gamma_{B_-} \Gamma_{B_+} \Gamma_A |\Gamma_C|^2 + |g|^2 |F_M|^2 (\Gamma_{B_+} + \Gamma_{B_-})}, \quad (30)$$

$$B_+ = -\frac{igF_A F_M \Gamma_B - \Gamma_C^*}{\Gamma_B - \Gamma_{B+} \Gamma_A |\Gamma_C|^2 + |g|^2 |F_M|^2 (\Gamma_{B+} + \Gamma_{B-})}. \quad (31)$$

Finally, for the pump mode we derive

$$A = \frac{\Gamma_B - \Gamma_{B+} |\Gamma_C|^2 F_A}{\Gamma_B - \Gamma_{B+} \Gamma_A |\Gamma_C|^2 + |g|^2 |F_M|^2 (\Gamma_{B+} + \Gamma_{B-})}. \quad (32)$$

To find the expressions for the output light we use Eq. (15) and derive

$$E_{\text{out-}} = -E_{\text{in}} \frac{2ig\gamma F_M^* \Gamma_{B+} \Gamma_C}{\Gamma_B - \Gamma_{B+} \Gamma_A |\Gamma_C|^2 + |g|^2 |F_M|^2 (\Gamma_{B+} + \Gamma_{B-})}, \quad (33)$$

$$E_{\text{out+}} = -E_{\text{in}} \frac{2ig\gamma F_M \Gamma_B - \Gamma_C^*}{\Gamma_B - \Gamma_{B+} \Gamma_A |\Gamma_C|^2 + |g|^2 |F_M|^2 (\Gamma_{B+} + \Gamma_{B-})}, \quad (34)$$

$$E_{\text{out}} = E_{\text{in}} \times \frac{\Gamma_B - \Gamma_{B+} (\Gamma_A - 2\gamma) |\Gamma_C|^2 + |g|^2 |F_M|^2 (\Gamma_{B+} + \Gamma_{B-})}{\Gamma_B - \Gamma_{B+} \Gamma_A |\Gamma_C|^2 + |g|^2 |F_M|^2 (\Gamma_{B+} + \Gamma_{B-})}. \quad (35)$$

Let us now calculate the power of the output light for the carrier wave  $W_0$  and the harmonics  $W_{\pm}$  with respect to the pump power  $W_{\text{in}}$ . For the sake of simplicity, we consider the entirely resonant case, i.e.,  $\Gamma_A = \Gamma_{B\pm} = \gamma$ ,  $\Gamma_C = \gamma_M$ . Introducing the quality factors as  $Q = \omega_0 / (2\gamma)$  and  $Q_M = \omega_M / (2\gamma_M)$ , and recalling that  $|C|^2 = |F_M|^2 / \gamma_M^2 = 4W_M Q_M / (\hbar \omega_M^2)$ , where  $W_M$  is the input microwave power, we derive the following expressions from Eqs. (33)–(35):

$$\frac{W_{\pm}}{W_{\text{in}}} = \left( \frac{2S}{1 + 2S^2} \right)^2, \quad (36)$$

$$\frac{W_0}{W_{\text{in}}} = \left( \frac{1 - 2S^2}{1 + 2S^2} \right)^2, \quad (37)$$

where

$$S = \frac{4|g|Q}{\omega_0} \left( \frac{W_M Q_M}{\hbar \omega_M^2} \right)^{1/2} \quad (38)$$

is the saturation parameter. Substituting Eq. (19) into Eq. (38), we obtain

$$S = Q \frac{16\pi\chi^{(2)}}{\epsilon_a} \left( \frac{2\pi W_M Q_M}{\epsilon_c \omega_M \nu_C} \right)^{1/2} \left( \frac{1}{\nu} \int_{\nu} d\nu \Psi_a \Psi_b \Psi_c \right). \quad (39)$$

Equations (36) and (37) tell us that there is an optimum value for the microwave power at which the conversion of the carrier frequency to the Stokes and anti-Stokes sidebands is most efficient. In principle, a complete conversion is possible for  $2S^2 = 1$ . In real experiments, however, a complete conversion does not happen because of the light and microwave power absorption. In our ide-

alized model the couplers, transmission lines, the optical cavity, and the microwave resonator are all assumed to be lossless. In particular, the decay terms account only for the transmission (and not absorption) of the fiber cavity couplers. Absorption will change Eqs. (8)–(10) that we used in our model.

In the experiments reported above we measured a photocurrent that is proportional to

$$I \sim |E_{\text{out}} + E_{\text{out}} - \exp(i\omega_M t) + E_{\text{out}} + \exp(-i\omega_M t)|^2. \quad (40)$$

The photocurrent resulting from the microwave carrier frequency is

$$I_M \sim (E_{\text{out}} E_{\text{out-}}^* + E_{\text{out}}^* E_{\text{out+}}) \exp(-i\omega_M t) + \text{c.c.}, \quad (41)$$

where c.c. stands for complex conjugation. Substituting Eqs. (33)–(35) into approximation (41) we can see that  $I_M$  is zero for the all-resonant case if  $g$  is real (pure phase modulation). The signal  $I_M$  is maximized if  $g$  is imaginary (amplitude modulation). In our case  $g$  is real.

We observe the modulation in the experiment because (i) the coupling of pump light and the cavity is not critical, i.e.,  $E_{\text{out}}$  has a constant bias compared with Eq. (35); (ii) we cannot exactly tune to the resonance of the loaded optical cavity or microwave resonator; and (iii) the cavity modes are not exactly equidistant. The calculated demodulated microwave power is shown in Fig. 10 as a function of laser detuning from the whispering-gallery-mode resonance. The plot is for an equidistant mode spectrum. We took into account that approximately 20% of the input light reflects from the coupling prism directly to the output channel and does not interact with the cavity because we do not have critical coupling. Therefore the output signal on the photodetector contains 20% of the nonmodulated light and 80% of the modulated light.

Let us estimate the interaction constant from Eq. (19). Taking  $\omega = 10^{15}$  rad/s,  $\omega_c = 7 \times 10^{10}$  rad/s,  $\chi^{(2)} = 10^{-11}$  m/V =  $3 \times 10^{-7}$  cgs (the value of the electro-optic constant does not coincide here with the value of the  $r_{33}$  constant for LiNbO<sub>3</sub> because the electric field of the

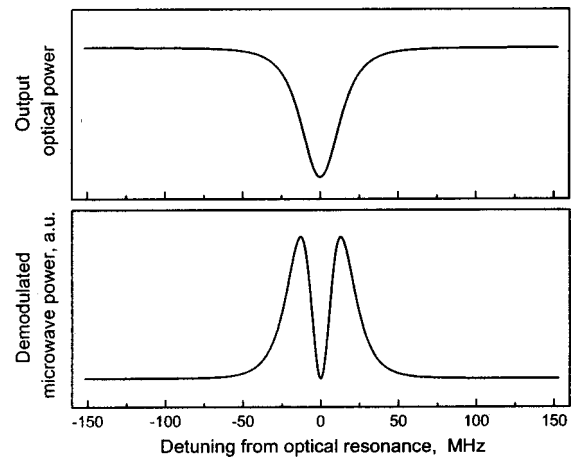


Fig. 10. Top: theoretically evaluated whispering-gallery-mode resonance. Bottom: theoretically evaluated demodulated microwave power versus detuning of the pump light from the whispering-gallery-mode resonance. No signal is found for the resonant tuning.

microwave cavity is not exactly collinear with the crystal axis),  $\mathcal{V}_c = 10^{-4} \text{ cm}^3$ , and the mode overlapping integral (...) = 0.5, we obtain  $g = 145 \text{ rad/s}$ .

In the experiment we have a maximum frequency conversion ( $S = 2^{-1/2}$ ) for  $W_M \approx 10 \text{ mW}$ ,  $Q_M \approx 100$ ,  $\omega_M \approx \omega_c$ , and  $Q \approx 10^6$ . This gives us  $g \approx 125 \text{ rad/s}$  [see Eq. (38)].

The difference between the measured and the calculated values of  $g$  can be explained when we allow for the imperfect mode overlap, absorption in the system, and the generation of additional harmonics that we did not take into account.

#### 4. MULTIPLE HARMONIC GENERATION

We have considered the case when interactions of light and microwave fields lead to the generation of two harmonics. This, however, is generally not the case, and multiple harmonic generation is possible if the cavity modes are equidistant in frequency and the distance between them is equal to the microwave frequency.

To describe harmonic generation we rewrite the interaction Hamiltonian as

$$\hat{V} = \hbar g \sum_{n=-\infty}^{\infty} (\hat{a}_{n-1}^\dagger \hat{c}^\dagger \hat{a}_n + \hat{a}_{n+1}^\dagger \hat{c} \hat{a}_n) + \text{adjoint}, \quad (42)$$

where  $\hat{a}_n$  is the annihilation operator for the  $n$ th cavity mode. We assume that modes are completely identical with respect to their quality factors and coupling strength to the microwave field.

Using Eq. (42) we derive the equations of motion for the modes. For the sake of simplicity we consider the case of exact resonance for all the modes. In slowly varying amplitude and phase approximation the equations for the expectation values of the field amplitudes are

$$\dot{A}_n = -\gamma A_n - ig(A_{n-1}C + C^*A_{n+1}) + F_A \delta_{n,0}, \quad (43)$$

$$\dot{C} = -\gamma_M C - ig \sum_{n=-\infty}^{\infty} (A_{n-1}^* A_n + A_n^* A_{n+1}) + F_M, \quad (44)$$

where  $F_A$  stands for the pump,  $\delta_{i,j} = 1$  if  $i = j$ , and  $\delta_{i,j} = 0$  if  $i \neq j$ . In other words, we assume that only a mode with  $\dot{n} = 0$  is pumped. Then  $A_{\pm 1}$  corresponds to  $B_{\pm}$  in our above consideration.

We assume that the set of Eqs. (43) and (44) has a steady-state solution:

$$\gamma A_n + ig(A_{n-1}C + C^*A_{n+1}) = F_A \delta_{n,0}, \quad (45)$$

$$\gamma_M C + ig \sum_{n=-\infty}^{\infty} (A_{n-1}^* A_n + A_n^* A_{n+1}) = F_M. \quad (46)$$

Equations (45) and (46) can be solved by Fourier transformation:

$$A(t) = \sum_{n=-\infty}^{\infty} A_n \exp(-i\omega_M n t). \quad (47)$$

In the case of exact resonance, the amplitude of the microwave field does not depend on the light intensity [see relation (29)]  $C = |F_M| \exp(i\phi_M)/\gamma_M$ . Then multiplying

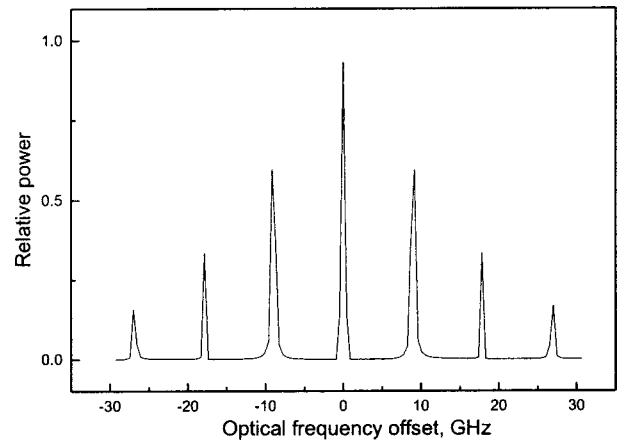


Fig. 11. Evaluated frequency spectrum of the modulated signal. Zero frequency corresponds to the carrier frequency of the pumping light.

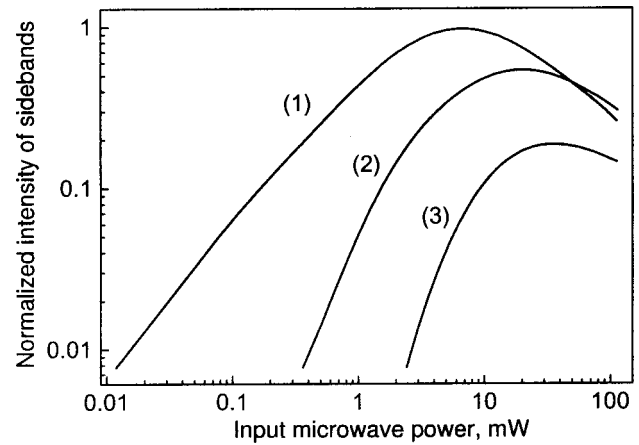


Fig. 12. Evaluated normalized power of optical harmonics generated in the modulator versus power of the microwave pump.

each term of Eq. (45) on  $\exp(-i\omega_M n t)$  ( $n$  corresponds to the index of the term  $\gamma A_n$ ) and summing them over all  $n$ , we derive

$$A(t) = \frac{F_A \gamma_M}{\gamma \gamma_M + 2ig|F_M| \cos(\omega_M t + \phi_M)}. \quad (48)$$

The solution for each mode  $A_n$  can be written as

$$A_n = \frac{1}{2\pi} \int_0^{2\pi/\omega_M} A(t) \exp(i\omega_M n t) dt. \quad (49)$$

To find the expression for the output light we use Eq. (15):

$$\begin{aligned} E_{\text{out}}(t) &= \frac{1 - 2iS \cos(\omega_M t + \phi_M)}{1 + 2iS \cos(\omega_M t + \phi_M)} E_{\text{in}}(t) \\ &= E_{\text{in}}(t) \exp\{-2i \arctan[2S \cos(\omega_M t + \phi_M)]\}. \end{aligned} \quad (50)$$

Therefore, in the case of multiple harmonics, the behavior of the system is different from the case of only three harmonics. An increase of the microwave power leads to the increase of the number of optical harmonics instead of the saturation and a decrease in the field amplitude, as was shown in Section 3.

We solve the set of Eqs. (45) and (46) for the same conditions as those used in Figs. 4 and 6. The result of the calculations are presented in Figs. 11 and 12. One can see a satisfactory correspondence between the experimental and the theoretical results.

## 5. DISCUSSION

Three-wave mixing is essentially a parametric process based on nonlinear media with  $\chi^{(2)}$  nonlinearity. This kind of wave mixing is not efficient in bulk materials because of the phase mismatch among the pump and the generated waves. The usual solution to this problem is the fabrication of artificially phase-matched materials.

This method, however, is not strictly applicable for intracavity nonlinear optics because the modes are orthogonal to each other in the momentum space, and the overlap integral for the modes taken over the entire cavity volume usually goes to zero. It is nonetheless possible to distribute a nonlinear medium in different regions of a cavity to avoid this problem. This solution, however, is difficult to implement when the cavity itself is constructed from a homogeneous nonlinear material, as is the whispering-gallery-mode cavity in our experiment.

As an alternative, we consider wave mixing of light and microwaves and use an optical cavity as well as a microwave resonator. In this way, instead of modifying the shape of a nonlinear medium, we modify the shape of the microwave resonator. The resonator covers only a half of the optical mode space and provides a variation of the microwave field over the perimeter. The mode overlap integral is nonzero in this case.

It is interesting to note that the mode orthogonality that causes problems with mode interaction also results in the useful effect of decreasing the noise in the system. Electro-optical crystals like  $\text{LiNbO}_3$  usually suffer from undesirable acoustic resonances because an electric field applied across a crystal induces stress by piezoelectricity. The induced stress gives rise to a strain, which in turn induces a change in the refractive index of the material through the photoelectric effect. Consequently the refractive index of a free electro-optic crystal changes in a complex manner that decreases the quality of the modulation.

To circumvent this problem, we use a small cavity fabricated from  $\text{LiNbO}_3$ . The cavity has a sparse acoustic as well as optical spectra. The acoustic modes themselves are usually orthogonal to the optical modes, and the strain induced in the material does not influence the light. In a similar manner, Brillouin scattering that usually decreases the performance of fiber-optic devices does not introduce any serious restriction in our case.

## 6. CONCLUSION

We propose theoretically, and implement experimentally, a configuration with high- $Q$  whispering-gallery modes excited in a nonlinear dielectric resonator to create an efficient mixing of light and microwave fields. We are able to overcome restrictions imposed by phase-matching conditions on the experimental realization of this process through engineering the geometries of the optical cavity

and microwave resonator. With this approach, we devise optical modulators and microwave receivers operating under a broad range of parameters. Our results are useful for practical as well as fundamental applications.

This research was carried out by the Jet Propulsion Laboratory, California Institute of Technology, under a contract with the National Aeronautics and Space Administration. A. A. Savchenkov also acknowledges support from National Research Council.

## REFERENCES AND NOTES

1. V. B. Braginsky, M. L. Gorodetsky, and V. S. Ilchenko, "Quality-factor and nonlinear properties of optical whispering gallery modes," *Phys. Lett. A* **137**, 393–397 (1989).
2. A. J. Campillo, J. D. Eversole, and H. B. Lin, "Cavity quantum electrodynamic enhancement of stimulated emission in microdroplets," *Phys. Rev. Lett.* **67**, 437–440 (1991).
3. L. Collot, V. Lefevre-Seguin, M. Brune, J.-M. Raimond, and S. Haroshe, "Very high- $Q$  whispering-gallery mode resonances observed in fused silica microspheres," *Europhys. Lett.* **23**, 327–334 (1993).
4. H. Mabuchi and H. J. Kimble, "Atom galleries for whispering atoms—binding atoms in stable orbits around an optical resonator," *Opt. Lett.* **19**, 749–751 (1994).
5. M. L. Gorodetsky, A. A. Savchenkov, and V. S. Ilchenko, "Ultimate  $Q$  of optical microsphere resonators," *Opt. Lett.* **21**, 453–455 (1996).
6. D. W. Vernooy, V. S. Ilchenko, H. Mabuchi, E. W. Streed, and H. J. Kimble, "High- $Q$  measurements of fused-silica microspheres in the near infrared," *Opt. Lett.* **23**, 247–249 (1998).
7. F. C. Blom, D. R. van Dijk, H. J. W. M. Hoekstra, A. Driessen, and T. J. A. Pompa, "Experimental study of integrated-optics microcavity resonators: toward an all-optical switching device," *Appl. Phys. Lett.* **71**, 747–749 (1997).
8. J. Popp, M. H. Fields, and R. K. Chang, " $Q$  switching by saturable absorption in microdroplets: elastic scattering and laser emission," *Opt. Lett.* **22**, 1296–1298 (1997).
9. J. E. Heebner and R. W. Boyd, "Enhanced all-optical switching by use of a nonlinear fiber ring resonator," *Opt. Lett.* **24**, 847–849 (1999).
10. H. M. Tzeng, K. F. Wall, M. B. Long, and R. K. Chang, "Laser emission from individual droplets at wavelengths corresponding to morphology-dependent resonances," *Opt. Lett.* **9**, 499–501 (1984).
11. J. C. Knight, H. S. T. Driver, R. J. Hutcheon, and G. N. Robertson, "Core-resonance capillary-fiber whispering-gallery-mode laser," *Opt. Lett.* **17**, 1280–1282 (1992).
12. V. Sandoghdar, F. Treussart, J. Hare, V. Lefevre-Seguin, J. M. Raimond, and S. Haroche, "Very low threshold whispering-gallery-mode microsphere laser," *Phys. Rev. A* **54**, R1777–R1780 (1996).
13. F. Treussart, V. S. Ilchenko, J. F. Roch, P. Domokos, J. Hare, V. Lefevre, J. M. Raimond, and S. Haroche, "Whispering gallery mode microlaser at liquid helium temperature," *J. Lumin.* **76**, 670–673 (1998).
14. F. Treussart, V. S. Ilchenko, J. F. Roch, J. Hare, V. Lefevre-Seguin, J. M. Raimond, and S. Haroche, "Evidence for intrinsic Kerr bistability of high- $Q$  microsphere resonators in superfluid helium," *Eur. Phys. J. D* **1**, 235–238 (1998).
15. M. Pelton and Y. Yamamoto, "Ultralow threshold laser using a single quantum dot and a microsphere cavity," *Phys. Rev. A* **59**, 2418–2421 (1999).
16. A. N. Oraevsky, M. O. Scully, T. V. Sarkisyan, and D. K. Bandy, "Using whispering gallery modes in semiconductor microdevices," *Laser Phys.* **9**, 990–1003 (1999).
17. M. Cai, O. Painter, K. J. Vahala, and P. C. Sercel, "Fiber-coupled microsphere laser," *Opt. Lett.* **25**, 1430–1432 (2000).

18. F. Lissillour, P. Feron, N. Dubreuil, P. Dupriez, M. Poulain, and G. M. Stephan, "Erbium-doped microspherical lasers at 1.56  $\mu\text{m}$ ," *Electron. Lett.* **36**, 1382–1384 (2000).
19. Y. S. Choi, H. J. Moon, K. Y. An, S. B. Lee, J. H. Lee, and J. S. Chang, "Ultrahigh- $Q$  microsphere dye laser based on evanescent-wave coupling," *J. Korean Phys. Soc.* **39**, 928–931 (2001).
20. V. S. Ilchenko and L. Maleki, "Novel whispering-gallery resonators for lasers, modulators, and sensors," in *Laser Resonators IV*, A. V. Kudryashov and A. H. Paxton, eds., Proc. SPIE **4270**, 120–130 (2001).
21. V. S. Ilchenko, M. L. Gorodetsky, X. S. Yao, and L. Maleki, "Microtorus: a high-finesse microcavity with whispering-gallery modes," *Opt. Lett.* **26**, 256–258 (2001).
22. W. von Klitzing, R. Long, V. S. Ilchenko, J. Hare, and V. Lefevre-Seguin, "Tunable whispering gallery modes for spectroscopy and CQED experiments," *New J. Phys.* **3**, 141–144 (2001).
23. S. Blair and Y. Chen, "Resonant-enhanced evanescent-wave fluorescence biosensing with cylindrical optical cavities," *Appl. Opt.* **40**, 570–582 (2001).
24. R. W. Boyd and J. E. Heebner, "Sensitive disk resonator photonic biosensor," *Appl. Opt.* **40**, 5742–5747 (2001).
25. K. Ohata, T. Inoue, M. Funabashi, A. Inoue, Y. Takimoto, T. Kuwabara, S. Shinozaki, K. Maruhashi, K. Hosaya, and H. Nagai, "Sixty-GHz-bang ultra-miniature monolithic T/R modules for multimedia wireless communication systems," *IEEE Trans. Microwave Theory Tech.* **44**, 2354–2360 (1996).
26. V. S. Ilchenko, X. S. Yao, and L. Maleki, "Microsphere integration in active and passive photonics devices," in *Laser Resonators III*; A. V. Kudryashov and A. H. Paxton, eds., Proc. SPIE **3930**, 154–162 (2000).
27. Toroidal cavity shape is essential here to obtain a large free spectral range (frequency splitting between neighboring cavity modes).
28. D. A. Cohen and A. F. J. Levi, "Microphotonic millimetre-wave receiver architecture," *Electron. Lett.* **37**, 37–39 (2001).
29. D. A. Cohen, M. Hossein-Zadeh, and A. F. J. Levi, "Microphotonic modulator for microwave receiver," *Electron. Lett.* **37**, 300–301 (2001).
30. D. A. Cohen and A. F. J. Levi, "Microphotonic components for a mm-wave receiver," *Solid-State Electron.* **45**, 495–505 (2001).
31. D. A. Cohen, M. Hossein-Zadeh, and A. F. J. Levi, "High- $Q$  microphotonic electro-optic modulator," *Solid-State Electron.* **45**, 1577–1589 (2001).
32. J. A. Stratton, *Electromagnetic Theory* (McGraw-Hill, New York, 1941).
33. H. M. Lai, P. T. Leung, K. Young, P. W. Barber, and S. C. Hill, "Time-independent perturbation for leaking electromagnetic modes in open system with application to resonances in microdroplets," *Phys. Rev. A* **41**, 5187–5198 (1990).
34. M. Abramowitz and I. A. Stegun, eds., *Handbook on Mathematical Functions* (Dover, New York, 1970).
35. D. F. Walls and G. J. Milburn, *Quantum Optics* (Springer, New York, 1994).
36. W. H. Louisell, A. Yariv, and A. E. Siegmann, "Quantum fluctuations and noise in parametric processes," *Phys. Rev.* **124**, 1646–1654 (1961).
37. J. A. Armstrong, N. Bloembergen, J. Ducuing, and P. S. Pershan, "Interactions between light waves in a nonlinear dielectric," *Phys. Rev.* **127**, 1918–1939 (1962).
38. R. Graham and H. Haken, "The quantum fluctuations of the optical parametric oscillator," *Z. Phys.* **210**, 276–302 (1968).